

Anomalous Photocurrent Reversal for the Same Polarization Direction in van der Waals Ferroelectric CuInP_2S_6


Yinxin Bai,^{1,§} Wei Hao,^{1,§} Yanghe Wang^{①,2,3,§}, Junjiang Tian,¹ Chuanshou Wang,¹ Yunlin Lei,¹ Yihao Yang,¹ Xiaodong Yao,¹ Qihang Liu,¹ Changjian Li,^{2,3,*} Mingqiang Gu,^{1,†} and Junling Wang^{1,3,4,‡}

¹Department of Physics, Southern University of Science and Technology, Shenzhen 518055, China

²Department of Materials Science and Engineering, Southern University of Science and Technology, Shenzhen 518055, China

³Guangdong Provincial Key Laboratory of Functional Oxide Materials and Devices, Southern University of Science and Technology, Shenzhen, China

⁴Department of Physics, City University of Hong Kong, Kowloon 999077, Hong Kong SAR, China

 (Received 20 October 2023; revised 7 January 2024; accepted 22 April 2024; published 21 May 2024)

The bulk photovoltaic effect (BPVE) in ferroelectric materials has attracted much attention due to its above-band-gap photovoltage and switchable photoresponse. However, the exact correlation between the photocurrent and spontaneous polarization remains unclear. Here, we report an anomalous reversal of the photocurrent, even for the same polarization direction, in van der Waals (vdW) ferroelectric CuInP_2S_6 (CIPS). Careful analysis reveals that the relocation of Cu ions into the vdW gap upon thickness reduction causes the current reversal, even though it does not change the polarization direction. By combining theoretical and experimental studies, we show clearly the decoupling of the BPVE photocurrent and electric polarization. This discovery significantly improves our understanding of the BPVE and demonstrates yet another example of the lattice dimensionality effect in vdW ferroelectrics.

DOI: [10.1103/PRXEnergy.3.023004](https://doi.org/10.1103/PRXEnergy.3.023004)

I. INTRODUCTION

The bulk photovoltaic effect (BPVE) is a second-order nonlinear optical effect that appears in crystals with broken inversion symmetry [1]. It was discovered more than half a century ago [2,3] and gained renewed interest in the past decade because of its above-band-gap photovoltage and potential to break the Shockley-Queisser limit [4,5]. Though not a necessary condition for the BPVE, the large reversible spontaneous polarizations of ferroelectric materials render them ideal platforms for investigating the fundamental physics and potential applications of the BPVE [6,7]. Advances in bandgap engineering and the discovery of other related phenomena, e.g., the flexophotovoltaic effect, further enrich the field [8–13].

It is now generally agreed that the BPVE arises due to the asymmetric shift of electron wave packets in real

space upon interband excitation by photons [14–17]. The shift vector, which describes the direction and magnitude of electron movement, is determined by the difference in the Berry connection of the Bloch wave functions of the two corresponding bands and only has a nonzero value in noncentrosymmetric systems. Since the polar axis represents the most asymmetric direction in a ferroelectric material, one may expect the photocurrent to be the largest along the polar axis and to follow a universal direction with respect to polarization. This, however, is not the case experimentally. For example, Nadupalli *et al.* reported that the bulk photocurrent was opposite to polarization in Fe-doped LiNbO_3 [18], while Abdelsamie *et al.* observed a photocurrent in the same direction as the polarization in BiFeO_3 [19]. Furthermore, the shift vector may not even be along the polar axis [20]. Wang *et al.* predicted that the shift current could be reversed due to ion displacement within a uniform polar state in the perovskite ferroelectrics [21], but there has been no experimental confirmation. Deciphering the correlation between the electron shift vector upon photon excitation and spontaneous polarization is essential for the design of ferroelectric-based optoelectronic devices. But the limited options for ion displacements in conventional ferroelectrics make the study very challenging, even though much effort has been devoted to the topic [21,22].

*Corresponding author: licj@sustech.edu.cn

†Corresponding author: gumq@sustech.edu.cn

‡Corresponding author: j.wang@cityu.edu.hk

§These authors contributed equally to this work.

Published by the American Physical Society under the terms of the [Creative Commons Attribution 4.0 International license](https://creativecommons.org/licenses/by/4.0/). Further distribution of this work must maintain attribution to the author(s) and the published article's title, journal citation, and DOI.

Recent developments in two-dimensional (2D) van der Waals (vdW) ferroelectrics [23] have sparked another wave of interest in the BPVE for multiple reasons. First of all, since the shift vector is related to the Berry curvature of Bloch bands, it is suggested that the BPVE can be enhanced in vdW Weyl semimetals (WSMs). For example, a large circularly polarized photogalvanic effect (CPGE) was observed in TaIrTe₄ recently; this is a type-II WSM [24]. Furthermore, it was predicted that the topological quantum Berry curvature of WSMs could host a quantized CPGE signal [25,26]. Second, from an engineering point of view, the high flexibility of vdW materials supports the flexophotovoltaic effect [12,13], an opportunity to be explored in future flexible electronic devices. Recently, a significant enhancement of the photocurrent by 2 orders of magnitude was reported in CuInP₂S₆ (CIPS) [27], presenting a promising route to surpass the Shockley-Queisser limit.

Here, we explore another unique feature of CIPS, i.e., the multiple stable locations of Cu ions within and outside of the vdW layer [28], to investigate the correlation between the shift current and spontaneous polarization. Surprisingly, besides a 6 times increase in the photocurrent amplitude, an anomalous photocurrent reversal occurs even for the same polarization direction when the CIPS thickness is reduced. Detailed analysis reveals that the spatial instability and relocation of Cu ions in CIPS due to its layered structure are responsible for this anomalous behavior, in agreement with first-principles calculations based on density functional theory (DFT). This is the first experimental evidence of the decoupling of electric polarization from the photocurrent direction in a uniform system, which significantly improves our understanding of the BPVE.

II. RESULT

A. Ferroelectric property of CIPS and the thickness-dependent phase transition

Bulk CIPS is a vdW ferroelectric material ($T_c \sim 315$ K) with a monoclinic structure (space group Cc). Each layer consists of an S framework with Cu, In, and P-P pairs filling the S octahedra alternately [Fig. 1(a)]. Due to the second-order Jahn-Teller effect, monovalent Cu ions tend to move away from the centers of the octahedra [28], leading to spontaneous polarization below about 315 K. Furthermore, it has been shown that Cu ions exist in multiple stable positions in the ferroelectric phase, which is related to the coupling between the Cu 4s and S *sp* orbitals across the vdW gap [29,30]. The four possible Cu sites are labeled Cu1, Cu2, Cu3, and Cu4, as shown in Fig. 1(a). Among them, Cu2 and Cu3 are located within the layer, while Cu1 and Cu4 are located on the vdW gap side of the S plane. The different locations of Cu ions (inside versus outside of the layer) lead to multiple spontaneous polarizations (low and high polarization states) [31] and different

longitudinal piezoelectric coefficients (d_{33}) [31,32]. Thus, the question naturally arises of how the shift current of CIPS would be affected by the different site occupancy of Cu ions.

To investigate the BPVE of CIPS, single crystals were grown using the chemical vapor transport method. X-ray diffraction (XRD) and Raman spectroscopy confirm the high quality of the crystals [Figs. S1(a)–S1(c) within the Supplemental Material [37]]. The UV-vis spectrum reveals a bandgap of 2.68 eV (~ 463 nm) at room temperature [Fig. S1(d) within the Supplemental Material [37]], consistent with a previous report [33]. As-grown CIPS crystals of 10–15 μm thick were sandwiched between bottom (20-nm Au) and top electrodes (20-nm Au) for electrical and optoelectrical measurements. The spontaneous polarization of CIPS is about 4 $\mu\text{C}/\text{cm}^2$ [Figs. 1(b) and S2(a) within the Supplemental Material [37]]. The retention test shows that the polarization is stable for at least 1 h [Fig. S2(b) within the Supplemental Material [37]], which is much longer than the photovoltaic measurement time.

Furthermore, to investigate the effect of multiple locations of Cu ions in CIPS due to its vdW structure, we take advantage of a recently reported structural phase transition from Cc to $P31c$ when its thickness is reduced [34]. We also verified the phase transition through transmission electron microscopy (TEM) [Figs. 1(c)–1(e)]. The TEM samples were prepared by dry transfer. Diffraction patterns along the [001] zone axis were obtained for samples of different thickness. The diffraction patterns of the thick and thin films match the simulated patterns for the Cc and $P31c$ space groups [Figs. 1(c)–1(e) and Fig. S3 within the Supplemental Material [37]], respectively, confirming a phase transition between 150 and 200 nm [Figs. 1(c)–1(e)]. Accompanying the phase transition, there is a relative in-plane shift of neighboring layers, and the Cu occupancy among the possible locations is affected; this is discussed in detail in Sec. II C.

B. Anomalous photocurrent reversal for the same polarization direction in CIPS

For photovoltaic measurements, symmetric Au electrodes were used to minimize contributions from the interface Schottky barriers and depolarization field. The samples were also poled into a single domain state before measurements to eliminate effects from ferroelectric domain walls [7]. We used a 445-nm laser as the excitation source for all photovoltaic measurements. If not particularly emphasized, the power density of light was 170 mW/cm^2 . A detailed experimental setup is shown in the inset of Fig. 2(e). The laser passes through a series of optics to obtain linearly polarized light with a continuously adjustable polarization direction and forms an angle φ with respect to the [010] axis in the b - c^* plane. $\theta = 90^\circ$ corresponds to the angle

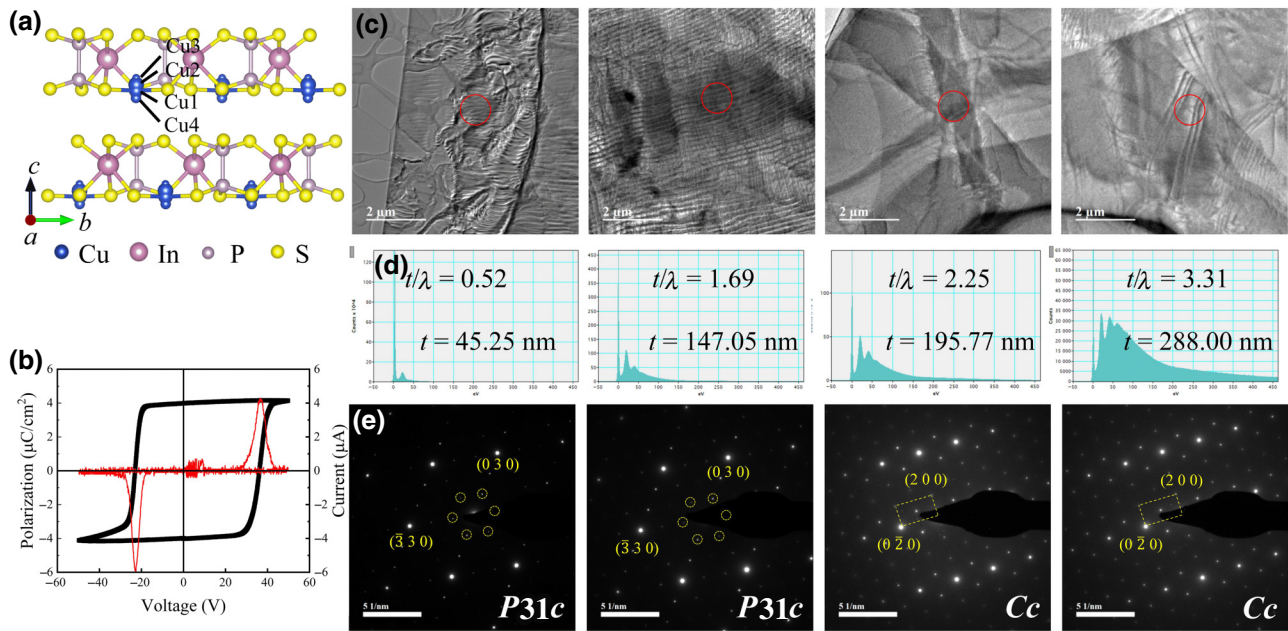


FIG. 1. (a) Crystal structure of CIPS in the Cc space group with the four Cu sites indicated. (b) Typical polarization-electric field hysteresis loop of a CIPS crystal ($\sim 15 \mu\text{m}$ thick) at room temperature. (c) Bright-field TEM images of CIPS films of different thicknesses. Red circle highlights the regions for SAED measurements. (d) Low-loss EELS spectra to estimate the thickness of the selected regions. From left to right, 45.25, 147.05, 195.77, and 288.00 nm. (e) SAED patterns of the selected areas.

between the electric field vector of light and the a axis of the sample [Fig. S4(b) within the Supplemental Material [37]]. Representative results obtained from a Au(20 nm)/CIPS(15 μm)/Au(20 nm) device are shown

in Fig. S5 within the Supplemental Material [37]. When the ferroelectric polarization is switched, the photocurrent also reverses. By changing the angle between the light polarization and the spontaneous polarization of CIPS,

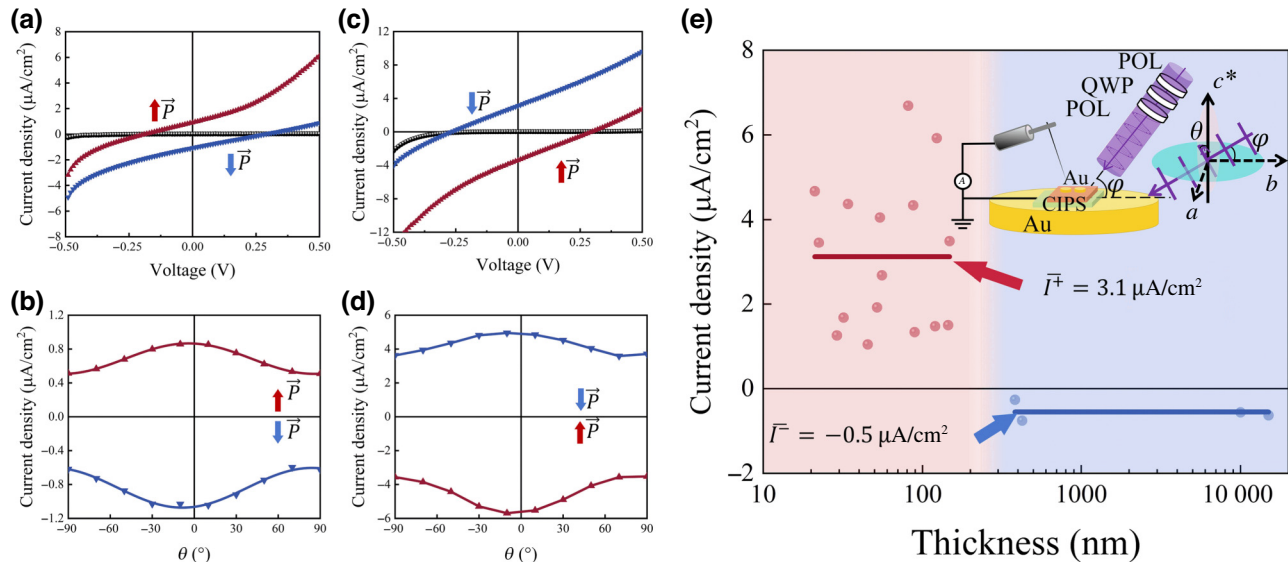


FIG. 2. Anomalous thickness dependence of the photovoltaic effect of CIPS. Photovoltaic response of two representative (a),(b) Au(20 nm)/CIPS(400 nm)/Au(20 nm) and (c),(d) Au(20 nm)/CIPS(87 nm)/Au(20 nm) devices. (e) $J = (J_{\text{down}} - J_{\text{up}})/2$ as a function of the CIPS thickness, showing the sharp transition at around 200 nm. J_{down} and J_{up} refer to the average values of photocurrents under different light polarization when the ferroelectric polarization is downward and upward, respectively. Inset, schematic illustration of the experimental setup used for the photovoltaic measurements. POL, Polarizer; QWP, Quarter-wave plate.

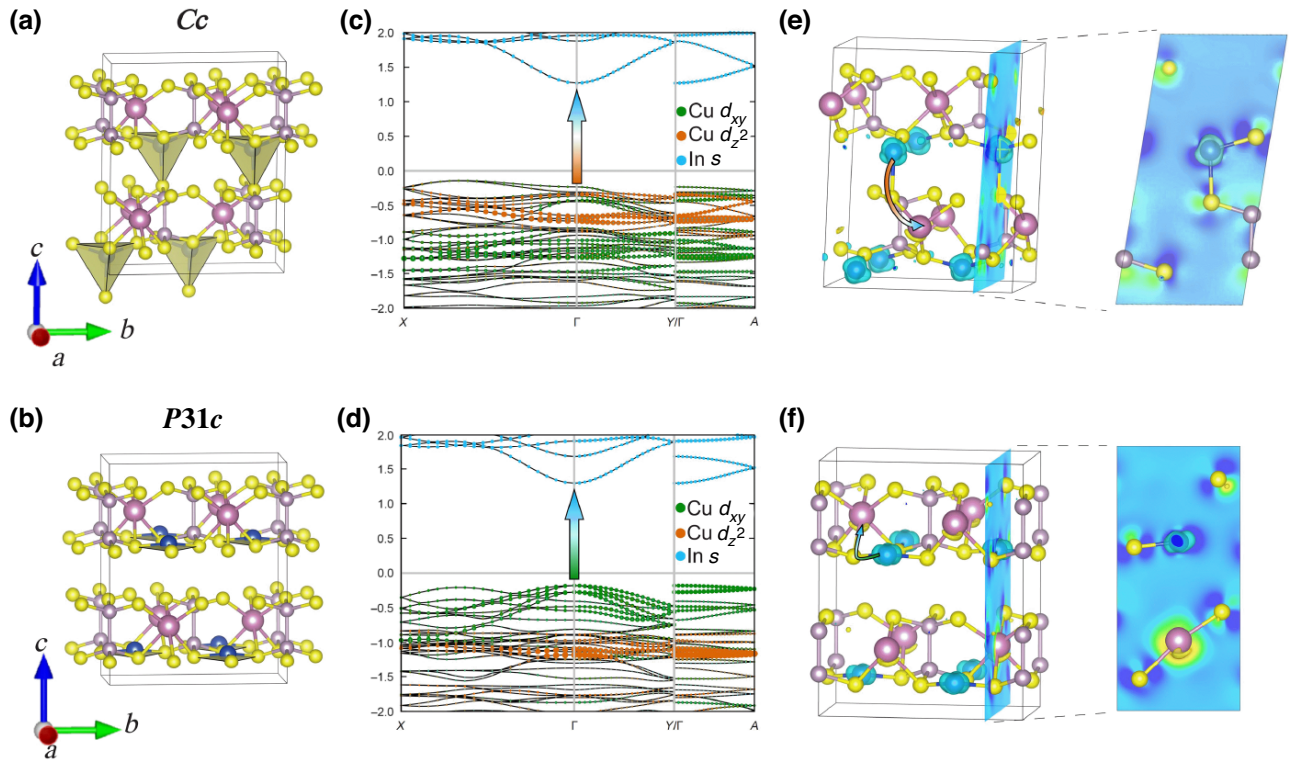


FIG. 3. Computed electronic structures of CIPS in Cc and $P31c$ phases. (a),(b) Crystal structures in these two phases for the downward polarization state. Cu-S tetrahedron and trigonal-planar ligands are highlighted. (c),(d) Band structures, with the contributions projected to the Cu d_{xy} (green), Cu d_{z^2} (orange), and In s (blue) orbitals. (e),(f) Charge density differences between the VBM and CBM. Arrows denote different excitation pathways in the two phases.

we observe sinusoidal behavior [Fig. S5(b) within the Supplemental Material [37]], which is the signature of the BPVE. By changing the angle φ and fitting the photocurrent curves following the BPVE model, we can obtain the BPVE coefficients (β_{31} , β_{32} , β_{33} , β_{35}) of CIPS (Fig. S6 within the Supplemental Material [37]), which are given in the Methods section within the Supplemental Material [37].

The photovoltaic behaviors of thin-film devices with CIPS thicknesses ranging between 20 and 400 nm were subsequently tested with φ kept at 30° . Interestingly, when the thickness of CIPS is greater than 200 nm, the BPVE is essentially the same as that of the bulk material [Figs. 2(a) and 2(b)]. However, when the thickness of CIPS drops below 200 nm, the direction of the photocurrent for the same polarization direction reverses completely [Figs. 2(c) and 2(d)]. In other words, the direction of the photocurrent changes from being opposite to the ferroelectric polarization direction to being in the same direction as the polarization. In addition, even though the photocurrents of different CIPS thin films are rather scattered, on average, they are about 6 times larger than that of the bulk [Fig. 2(e)], consistent with a previous report [27]. However, the sudden reversal of the photocurrent upon reducing the CIPS thickness has not been reported before.

C. Modeling and theoretical calculations

Why would the photocurrent direction reverse for the same polarization direction? To answer this question, we need to look at the atomic details of the two structures. Previous studies revealed that Cu in CIPS had four possible locations, in which the interlayer locations [Cu1 and Cu4 in Fig. 1(a)] were correlated with the hybridization of the $4s$ orbitals of Cu and the sp orbitals of S ions in the adjacent layer. Take the downward polarization state as an example. In this state, the Cu ions are located near the lower S plane of the vdW layer. In the bulk Cc phase, the Cu ions are right on top of the S ions of the adjacent layer. Cu and the four surrounding S ions form a CuS_4 tetragonal ligand [Fig. 3(a)], and the Cu1 and Cu4 positions are metastable, causing some Cu ions to move into the vdW gap between two layers. When CIPS changes from the Cc phase to the $P31c$ phase, there is an in-plane shift between adjacent layers, causing the Cu ions at the upper layer to move sideways with respect to the S ions of the lower layer. CuS_3 trigonal-planar ligands, instead of CuS_4 , are formed, resulting in most Cu ions moving into the Cu2 and Cu3 sites within the layer [Fig. 3(b)]. This is confirmed by DFT calculations (Fig. S8 within the Supplemental Material [37]). Note that such relocations of Cu ions do not flip the ferroelectric polarization because

all these sites are around the same (lower) S plane of the layer.

The changes in microstructure across the phase transition, especially the subtle displacement of Cu ions, can affect the electronic structure of CIPS and eventually lead to the reversal of photocurrent. Specifically, the valence-band maximum (VBM) of CIPS is mainly composed of the $3d$ orbitals of Cu ions at the Γ point, while the conduction-band minimum (CBM) is contributed to by the $5s$ orbitals of In and the $3p$ orbitals of S ions. Comparing Figs. 3(c) and 3(d), one can find that there is a significant out-of-plane Cu d_{z^2} orbital contribution to the VBM in the Cc phase, which is highly suppressed in the $P31c$ phase, leaving only the in-plane Cu d_{xy} component. The change in the VBM component leads to a different electron distribution in real space. Figures 3(e) and 3(f) display the charge density difference between the CBM and the VBM, revealing distinct electron transfer pathways between the two phases during optical excitation. In the $P31c$ phase, electron excitation occurs from Cu to In through the three S ions within the same layer. As depicted by the blue-colored electron cloud on the left of Fig. 3(f), this leads to electron loss by a Cu ion predominantly confined within the x - y plane. On the other hand, due to the existence of a Cu-S bond along the z direction in the Cc phase, the electron loss cloud for the Cu ion exhibits notable deformations and out-of-plane components. Since the shift current associated with the BPVE originates from the change in the center of mass when electrons are excited from the VBM to the CBM [1,12,16,22,35], the difference in electron excitation channels between the two Cu ion locations eventually leads to the reversal of the shift current direction upon the phase transition. In other words, in the $P31c$ phase, electron excitation from Cu to In through the S ions within the same layer supports a photocurrent in the $+z$ direction, whereas in the Cc phase, the interlayer Cu-S-In charge transfer (besides intralayer transfer) during excitation results in a $-z$ component. The computed shift current components σ_{zy} and σ_{zz} for Cu occupying sites 2 and 4 (in the Cc phase) indeed confirm this prediction (Fig. S9 within the Supplemental Material [37]).

This model also explains the increase in photocurrent upon reducing the thickness of CIPS. It has been reported that in bulk CIPS (Cc phase), the occupancy probabilities for Cu1 + Cu4 and Cu2 + Cu3 are comparable [30]. The shift currents of these two states are in opposite directions, thus canceling mostly each other out. In the thin films ($P31c$ phase), Cu mostly occupies the Cu2 site within the layers, leading to a much larger photocurrent.

III. DISCUSSION

In summary, we have observed an anomalous reversal of the photocurrent direction for the same polarization direction in CIPS when its thickness is reduced to

below about 200 nm; this provides clear evidence of the decoupling between the BPVE photocurrent and electric polarization of the system. Careful structural analysis and first-principles calculations reveal that a structural phase transition occurs upon reducing the thickness of CIPS. More importantly, the occupancy of Cu ions among the four possible locations changes between these two phases, affecting the shifting direction of the electron mass center in real space when electrons are excited from the VBM to the CBM. The correlation between photocurrent direction and bonding states significantly improves our understanding of the BPVE and the shift current model, and the discovery demonstrates yet another example of the lattice dimensionality effect brought about by the layered structure of vdW ferroelectrics.

All data needed to evaluate the conclusions in the paper are present in the paper and/or the Supplemental Material.

ACKNOWLEDGMENTS

We acknowledge support from the Guangdong Innovative and Entrepreneurial Research Team Program (Grant No. 2021ZT09C296), the National Natural Science Foundation of China (Grant No. 12074164), the National Key Research and Development of China (No. 2022YFA1402903), and the Guangdong Provincial Key Laboratory Program (2021B1212040001) from the Department of Science and Technology of Guangdong Province. M.G. was supported by the Natural Science Foundation of Guangdong Province (2021A1515110389) and the Science Technology and Innovation Commission of Shenzhen Municipality (JCYJ20210324104812034). C.L. acknowledges financial support from the National Natural Science Foundation of China (52172115); the Natural Science Foundation of Guangdong Province (2022A1515010762); and the Guangdong Provincial Department of Education Innovation Team Program (2021KCXTD012).

J.W. and Y.B. conceived the idea and designed the study. W.H. and M.G. performed the DFT calculations. Y.W. and C.L. performed TEM analysis. All authors contributed to the discussion of the results and writing of the manuscript.

The authors declare no competing financial interests.

-
- [1] B. I. Sturman and V. M. Fridkin, *The Photovoltaic and Photorefractive Effects in Noncentrosymmetric Materials* (Routledge, London, 2021).
 - [2] W. T. H. Koch, R. Munser, W. Ruppel, and P. Wurfel, Anomalous photovoltage in BaTiO₃, *Ferroelectrics* **13**, 305 (1976).
 - [3] A. M. Glass, D. von der Linde, D. H. Auston, and T. J. Negran, Excited state polarization, bulk photovoltaic effect and the photorefractive effect in electrically polarized media, *J. Electron. Mater.* **4**, 915 (1975).

- [4] J. E. Spanier, V. M. Fridkin, A. M. Rappe, A. R. Akbashev, A. Polemi, Y. Qi, Z. Gu, S. M. Young, C. J. Hawley, D. Imbrenda, *et al.*, Power conversion efficiency exceeding the Shockley–Queisser limit in a ferroelectric insulator, *Nat. Photonics* **10**, 611 (2016).
- [5] W. Shockley and H. J. Queisser, Detailed balance limit of efficiency of p - n junction solar cells, *J. Appl. Phys.* **32**, 510 (1961).
- [6] T. Choi, S. Lee, Y. J. Choi, V. Kiryukhin, and S. W. Cheong, Switchable ferroelectric diode and photovoltaic effect in BiFeO₃, *Science* **324**, 5923 (2009).
- [7] S. Y. Yang, J. Seidel, S. J. Byrnes, P. Shafer, C. H. Yang, M. D. Rossell, P. Yu, Y. H. Chu, J. F. Scott, J. W. Ager, *et al.*, Above-bandgap voltages from ferroelectric photovoltaic devices, *Nat. Nanotechnol.* **5**, 143 (2010).
- [8] I. Grinberg, D. V. West, M. Torres, G. Gou, D. M. Stein, L. Wu, G. Chen, E. M. Gallo, A. R. Akbashev, P. K. Davies, *et al.*, Perovskite oxides for visible-light-absorbing ferroelectric and photovoltaic materials, *Nature* **503**, 509 (2013).
- [9] R. Nechache, C. Harnagea, S. Li, L. Cardenas, W. Huang, J. Chakrabarty, and F. Rosei, Bandgap tuning of multiferroic oxide solar cells, *Nat. Photonics* **9**, 61 (2014).
- [10] M. M. Yang, D. J. Kim, and M. Alexe, Flexo-photovoltaic effect, *Science* **360**, 6391 (2018).
- [11] Y. J. Zhang, T. Ideue, M. Onga, F. Qin, R. Suzuki, A. Zak, R. Tenne, J. H. Smet, and Y. Iwasa, Enhanced intrinsic photovoltaic effect in tungsten disulfide nanotubes, *Nature* **570**, 349 (2019).
- [12] J. Jiang, Z. Chen, Y. Hu, Y. Xiang, L. Zhang, Y. Wang, G. C. Wang, and J. Shi, Flexo-photovoltaic effect in MoS₂, *Nat. Nanotechnol.* **16**, 894 (2021).
- [13] Y. Dong, M. M. Yang, M. Yoshii, S. Matsuoka, S. Kitamura, T. Hasegawa, N. Ogawa, T. Morimoto, T. Ideue, and Y. Iwasa, Giant bulk piezophotovoltaic effect in 3R-MoS₂, *Nat. Nanotechnol.* **18**, 36 (2023).
- [14] S. M. Young, F. Zheng, and A. M. Rappe, First-principles calculation of the bulk photovoltaic effect in bismuth ferrite, *Phys. Rev. Lett.* **109**, 236601 (2012).
- [15] S. M. Young and A. M. Rappe, First principles calculation of the shift current photovoltaic effect in ferroelectrics, *Phys. Rev. Lett.* **109**, 116601 (2012).
- [16] B. I. Sturman, Ballistic and shift currents in the bulk photovoltaic effect theory, *Phys-Usp* **63**, 407 (2020).
- [17] Z. Dai and A. M. Rappe, Recent progress in the theory of bulk photovoltaic effect, *Chem. Phys. Rev.* **4**, 011303 (2023).
- [18] S. Nadupalli, J. Kreisel, and T. Granzow, Increasing bulk photovoltaic current by strain tuning, *Sci. Adv.* **5**, 3 (2019).
- [19] A. Abdelsamie, L. You, L. Wang, S. Z. Li, M. Q. Gu, and J. L. Wang, Crossover between bulk and interface photovoltaic mechanisms in a ferroelectric vertical heterostructure, *Phys. Rev. Appl.* **17**, 024047 (2022).
- [20] W. Ji, K. Yao, and Y. C. Liang, Evidence of bulk photovoltaic effect and large tensor coefficient in ferroelectric BiFeO₃ thin films, *Phys. Rev. B* **84**, 094115 (2011).
- [21] F. Wang, S. M. Young, F. Zheng, I. Grinberg, and A. M. Rappe, Substantial bulk photovoltaic effect enhancement via nanolayering, *Nat. Commun.* **7**, 10419 (2016).
- [22] M. Nakamura, S. Horiuchi, F. Kagawa, N. Ogawa, T. Kurumaji, Y. Tokura, and M. Kawasaki, Shift current photovoltaic effect in a ferroelectric charge-transfer complex, *Nat. Commun.* **8**, 281 (2017).
- [23] C. Wang, L. You, D. Cobden, and J. Wang, Towards two-dimensional van der Waals ferroelectrics, *Nat. Mater.* **22**, 542 (2023).
- [24] J. Ma, Q. Gu, Y. Liu, J. Lai, P. Yu, X. Zhuo, Z. Liu, J. H. Chen, J. Feng, and D. Sun, Nonlinear photoresponse of type-II Weyl semimetals, *Nat. Mater.* **18**, 476 (2019).
- [25] A. M. Cook, B. M. Fregoso, F. de Juan, S. Coh, and J. E. Moore, Design principles for shift current photovoltaics, *Nat. Commun.* **8**, 14176 (2017).
- [26] F. de Juan, A. G. Grushin, T. Morimoto, and J. E. Moore, Quantized circular photogalvanic effect in Weyl semimetals, *Nat. Commun.* **8**, 15995 (2017).
- [27] Y. Li, J. Fu, X. Mao, C. Chen, H. Liu, M. Gong, and H. Zeng, Enhanced bulk photovoltaic effect in two-dimensional ferroelectric CuInP₂S₆, *Nat. Commun.* **12**, 5896 (2021).
- [28] V. Maisonneuve, V. B. Cajipe, A. Simon, R. VonDerMuhll, and J. Ravez, Ferrielectric ordering in lamellar CuInP₂S₆, *Phys. Rev. B* **56**, 10860 (1997).
- [29] S. Zhou, L. You, A. Chaturvedi, S. A. Morris, J. S. Herrin, N. Zhang, A. Abdelsamie, Y. Z. Hu, J. Q. Chen, Y. Zhou, *et al.*, Anomalous polarization switching and permanent retention in a ferroelectric ionic conductor, *Mater. Horiz.* **7**, 263 (2020).
- [30] L. You, Y. Zhang, S. Zhou, A. Chaturvedi, S. A. Morris, F. Liu, L. Chang, D. Ichinose, H. Funakubo, W. Hu, *et al.*, Origin of giant negative piezoelectricity in a layered van der Waals ferroelectric, *Sci. Adv.* **5**, 4 (2019).
- [31] J. A. Brehm, S. M. Neumayer, L. Tao, A. O’Hara, M. Chyasnachichus, M. A. Susner, M. A. McGuire, S. V. Kalinin, S. Jesse, P. Ganesh, *et al.*, Tunable quadrupole-well ferroelectric van der Waals crystals, *Nat. Mater.* **19**, 43 (2020).
- [32] S. M. Neumayer, L. Tao, A. O’Hara, J. Brehm, M. W. Si, P. Y. Liao, T. L. Feng, S. V. Kalinin, P. D. D. Ye, S. T. Pantelides, *et al.*, Alignment of polarization against an electric field in van der Waals ferroelectrics, *Phys. Rev. Appl.* **13**, 064063 (2020).
- [33] I. P. Studenyak, V. V. Mitrovcij, G. S. Kovacs, M. I. Gurzan, O. A. Mykajlo, Y. M. Vysochanskii, and V. B. Cajipe, Disordering effect on optical absorption processes in CuInP₂S₆ layered ferroelectrics, *Phys. Status Solidi B* **236**, 678 (2003).
- [34] J. Deng, Y. Liu, M. Li, S. Xu, Y. Lun, P. Lv, T. Xia, P. Gao, X. Wang, and J. Hong, Thickness-dependent in-plane polarization and structural phase transition in van der Waals ferroelectric CuInP₂S₆, *Small* **16**, 1904529 (2020).
- [35] L. Z. Tan, F. Zheng, S. M. Young, F. G. Wang, S. Liu, and A. M. Rappe, Shift current bulk photovoltaic effect in polar materials—hybrid and oxide perovskites and beyond, *npj Comput. Mater.* **2**, 16026 (2016).
- [36] M. Klinger and A. Jäger, Crystallographic tool box (CrysT-Box): Automated tools for transmission electron microscopists and crystallographers, *J. Appl. Crystallogr.* **48**, 2012 (2015).
- [37] See the Supplemental Material at <http://link.aps.org/supplemental/10.1103/PRXEnergy.3.023004> for details of material characterization, the experimental setup, device photovoltaic characterization, and relevant computational results.